Subtype Specific Effects of Peroxisome Proliferator-Activated Receptor Ligands on Corepressor Affinity

Thomas B. Stanley,*,‡ Lisa M. Leesnitzer,§ Valerie G. Montana,|| Cristin M. Galardi,# Millard H. Lambert,|| Jason A. Holt,# H. Eric Xu,||,⊥ Linda B. Moore,§ Steven G. Blanchard,§ and Julie B. Stimmel§

Gene Expression and Protein Biochemistry, Systems Research, Computational, Analytical, and Structural Sciences and High Throughput Biology, Nuclear Receptor Discovery Research, GlaxoSmithKline Research and Development, Research Triangle Park, North Carolina 27709

Received March 24, 2003; Revised Manuscript Received May 14, 2003

ABSTRACT: Natural ligands for nuclear receptors are believed to activate gene transcription by causing dissociation of corepressors and promoting the association of coactivator proteins. Using multiple biophysical techniques, we find that peptides derived from one of the nuclear receptor interacting motifs of the corepressors nuclear receptor corepressor (NCoR) and silencing mediator of retinoid and thyroid receptors (SMRT) are able to bind the ligand binding domains (LBD) of all three PPAR (peroxisome proliferator activated receptor) subtypes. Using these peptides as tools, we find that ligands designed as selective agonists for PPARγ promote the association of coactivator peptides and dissociation of corepressor peptides as expected on PPARγ but surprisingly have varied effects on the binding of corepressor peptides to the other PPAR subtypes. In particular, some members of a class of L-tyrosine-based compounds designed as selective agonists for PPARγ reduce the affinity for corepressor peptides on PPARγ but increase the affinity for the same peptides on PPARδ and in one case on PPARα. We provide structural data that suggests that the molecular basis for these observations are variations in the ligand binding pockets of the three PPAR subtypes that are perturbed differentially by individual ligands and result in altered presentations of the overlapping coactivator/corepressor binding surfaces.

Peroxisome proliferator activated receptors (PPARs)[1] are transcription factors of the nuclear receptor family that are believed to be involved in the regulation of glucose, lipid, and cholesterol levels (for recent review, see ref *1*). The natural ligands for PPARs are thought to be fatty acids and their derivatives. There are three subtypes of PPARs: PPARα (NR1C1), PPARδ (NR1C2), and PPARγ (NR1C3). All three subtypes share a domain organization common of other nuclear receptors with a highly conserved N-terminal DNA binding domain and a moderately conserved C-terminal ligand binding domain (LBD). The PPARs are important regulators in multiple metabolic pathways that include fatty acid and carbohydrate metabolism. PPARα is the target for lipid lowering fibrate drugs (*2*), while PPARγ is the target for antidiabetic agents of the thiazolidinedione (TZD) class that includes troglitazone, pioglitazone, and rosiglitazone (*3*). In addition, novel tyrosine-based PPARγ ligands have been described that are potent insulin sensitizers and in some cases are highly selective for PPARγ in binding and functional cell-based assays (*4*−*7*). Recent evidence suggests that PPARδ-selective ligands may promote reverse cholesterol transport and thereby decrease cardiovascular disease associated with metabolic syndrome X (*8*).

Ligands exert their effects on gene transcription primarily through ligand-mediated binding of coactivator or corepressor proteins to nuclear receptors. An increasing number of coactivator proteins have been identified for nuclear receptors, of which a number have been implicated in the regulation of PPARs. These include SRC/p160 family (*9*, *10*) CBP/p300 (*11*) that have inherent histone acetylase activity and remodel chromatin structure as well as coactivators such as TRAP220/DRIP205 (*12*, *13*), which interact with the basal transcriptional machinery. Most of these coactivators possess one or more nuclear receptor interaction domains composed of a conserved LXXLL motif that mediate the interaction of the coactivator with the LBD of the nuclear receptor (*14*, *15*). In the unliganded state, or in some cases, the presence of antagonists, many nuclear receptors are complexed with corepressor proteins that repress transcription, apparently via an associated histone-deacetylase activity (*16*−*18*). The addition of a classical agonist ligand promotes the dissociation of the corepressor and the binding of coactivator proteins resulting in an enhancement in the basal level of transcription of specific genes (*19*−*22*). Altered interactions of nuclear receptors with

* To whom correspondence should be addressed. Telephone: (919) 483-0025. Fax: (919) 483-0368. E-mail: thomas.b.stanley@gsk.com.
‡ Gene Expression and Protein Biochemistry.
§ Systems Research.
|| Computational, Analytical, and Structural Sciences.
High Throughput Biology.
⊥ Current address: Laboratory of Structural Sciences, Van Andel Research Institute, Grand Rapids, MI 49503.

[1] Abbreviations: APC, allophycocyanin; CBP, CREB binding protein; DTT, dithiothreitol; FRET, fluorescence resonance energy transfer; HEPES, *N*-(2-hydroxyethyl)piperazine-*N*′-2-ethanesulfonic acid; LBD, ligand binding domain; NCoR, nuclear receptor corepressor; PPAR, peroxisome proliferator activated receptor; SMRT, silencing mediator of retinoid and thyroid receptors; SPAP, secreted placental alkaline phosphatase; TZD, thiazolidinedione; TR, thyroid receptor; TRIS, tris(hydroxymethyl)aminomethane.

10.1021/bi034472c CCC: $25.00
Published on Web 07/15/2003

corepressor proteins have been implicated in a number of disease states and pathologies such as thyroid hormone resistance syndromes, promyelocytic leukemia, and perhaps tamoxifen resistant breast cancer (*23*−*26*).

Two of the better characterized corepressors are: nuclear receptor corepressor (NCoR) and silencing mediator for retinoid and thyroid receptors (SMRT). The binding sites for nuclear receptors have been localized to homologous domains within the C-termini of both NCoR and SMRT (*27*−*29*). Nuclear receptor binding motifs analogous to the LXXLL found for coactivators have been identified for corepressors. Several labs have identified multiple (I/L)XX-(I/V)I motifs in the C-terminal region of both NCoR and SMRT that mediate the interactions with nuclear receptors (*27*, *29*−*31*). Others have suggested that the corepressor motif is extended and includes an additional hydrophobic residue to give a LXXXIXXX(L/I) motif (*28*). We have recently presented both biochemical and structural data that indicate the corepressor motif is an extended LXXXIXXX-(L/I) motif when bound to PPARα (*32*). Correct positioning of the AF2 helix at the C-terminal end of the PPAR LBDs by agonist ligands is essential for nuclear receptor activation by enhancing the affinity for the LXXLL motif of coactivator proteins. The extended corepressor motif occupies the same space as both the coactivator and the active position of the AF2 helix. Therefore, a ligand that displaces the AF2 helix from its active position would be expected to facilitate the interaction with corepressor proteins and is one potential mechanism for repression of nuclear receptor activity (*32*).

The structures of the LBDs of all three PPAR receptor subtypes have been solved (*15*, *33*, *34*−*36*) and indicate that key residues in the ligand binding pockets are responsible for ligand selectivity among subtypes and may be responsible for the specific pharmacologies of the different receptor subtypes (*37*). These studies have shown that PPARs have substantially larger ligand binding pockets than other nuclear receptors, which allow PPARs to bind a wide variety of ligands. Agonist structures of PPARγ with the thiazolidinedione, rosiglitazone (*15*), the tyrosine-based ligand farglitazar (GI262570) (*33*), as well as the dual PPARα/PPARγ tyrosine-based GW9544 (*36*), have been described. These structures reveal that the molecular switch for activating the PPAR receptors is a hydrogen bond between a Tyr in the AF2 helix and the carboxyl headgroups of both rosiglitazone and the tyrosine-based compounds that orients the AF2 helix in the active conformation.

Nuclear receptor/cofactor interactions may play important roles in the pathology of disease. Therefore, an understanding of the molecular mechanism of these interactions is essential for understanding nuclear receptor biology and the design of nuclear receptor targeted therapies. Previous studies have used peptides and fragments of coactivators to profile the effects of ligands on coactivator recruitment to the estrogen receptors (*38*−*40*). We have extended this concept by including corepressor peptides to obtain a more complete profile of a ligand by assessing not only their effect on coactivator affinity but corepressor affinity as well. To this end, we have used peptides derived from natural coactivator and corepressor sequences containing the characteristic LXXLL or LXXXIXXX(L/I) motif as models to measure the effect of ligands on the interaction of these peptides with the three PPAR subtypes. Using multiple biophysical techniques, we find that PPAR agonists increase the binding to peptides derived from coactivators but have varied effects on corepressor peptide association to the three PPAR subtypes. Results from a mammalian 2-hybrid cell-based interaction assay using full-length PPAR subtypes and fragments derived from coactivator and corepressor proteins were consistent with results obtained using peptides. The molecular mechanisms for these effects are differences in how diverse ligands occupy the ligand binding pockets of the PPAR subtypes, resulting in altered presentation of the coactivator/corepressor binding surface. These results suggest that different compound classes may have different PPAR subtype specificities and biological effects depending on the coactivator/corepressor context of the target tissue.

MATERIALS AND METHODS

Reagents. The following compounds were synthesized by the Medicinal Chemistry Department at GlaxoSmithKline: GW7845 (*6*), GW1929 (*4*), GW1516 (*8*), and GW9544 (*36*). Rosiglitazone and pioglitazone were synthesized according to published procedures. The following peptides were ordered from SynPep (Dublin, CA). NCoR ID-C (residues 2251−2275; Genbank accession NP_006302): (biotin-GHSFAD-PASNLGLEDIIRKALMGSF-$CONH_2$, fluoroscein-GHS-FADPASNLGLEDIIRKALMGSF) and SMRT ID-C (residues 2338−2361; Genbank accession XP_045602): (fluoroscein-TNMGLEAIIRKALMGKYDQWEE).

Protein Expression. CREB binding protein (CBP, residues 57−454; GenBank accession S39162), the LBDs of PPARα (residues 192−468; Genbank accession S74349), human PPARδ (residues 139−441; Genbank accession L07592), human PPARγ (residues 206−477; Genbank accession L40904), and TRβ (residues 202−456; Genbank accession P10828) containing a MKKGHHHHHHG were expressed in bacterial (BL21-DE3) cells using the plasmid vector pRSETA and purified as described previously (*41*). Protein and peptide concentrations were determined by quantitative amino acid analysis by subjecting peptides to gas-phase hydrolysis with 6 N HCl for 1 h at 15 °C, followed by amino acid analysis using a Waters AccQ-Tag amino acid analysis system as described previously (*42*).

Binding of Nuclear Receptor LBDs to Corepressor Peptides by Fluorescence Polarization. All experiments were conducted with buffer containing 10 mM HEPES pH 7.4, 0.15 M NaCl, 3 mM EDTA, 0.005% polysorbate-20 5 mM DTT, and 2% DMSO. Varied concentrations of receptor were incubated at room temperature with 10 nM of fluorescein-labeled NCoR ID-C or SMRT ID-C peptide. The fluorescence polarization values for each concentration of receptor were determined using a Packard Fusion α fluorescence plate reader with 485 nm excitation and 520 nm emission filters. Binding isotherms were constructed, and apparent K_D values were determined by nonlinear least-squares fit of the data to an equation for a simple 1:1 interaction. Reported K_D values are the average of at least two independent experiments.

Fluorescence Energy Transfer Assay. Fluorescently labeled PPARs and coactivator and corepressor reagents were prepared as described previously (*41*). Europium-labeled PPAR receptor (10 nM), APC-labeled NCoR or CBP, and ligand were mixed in individual wells of 96-well plates. The

Scheme 1

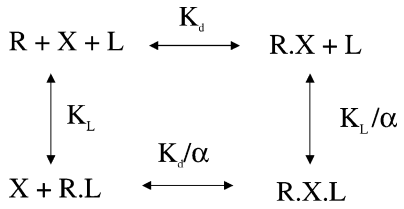

concentration of CBP ranged from 25 to 150 nM, and the concentration of NCoR ranged from 100 to 250 nM. The plates were incubated for at least 3 h at room temperature. Time-resolved fluorescence intensities were determined in a Victor 1420 Multilabel Counter. Plots of fluorescence intensity ratio (intensity at 665 nm/intensity at 610 nm) versus ligand concentration were constructed. Dose response curves were done in duplicate at each cofactor concentration.

Experimental data were fit to a model based in Scheme 1 using the equations below (derivations in the Supporting Information) by a nonlinear least squares algorithm (typically using Microsoft Excel or SigmaPlot).

$$F = q_0 + q_1\left(\frac{\nu - \sqrt{\nu^2 - 4R_0X_0}}{2}\right)$$

where

$$\nu = \left(X_0 + R_0 + K_d\left[\frac{K_L + L_0}{K_L + \alpha L_0}\right]\right)$$

Ligand and cofactor concentrations (L_0 and X_0, respectively) served as independent variables and observed fluorescence, F, was the dependent variable. The total receptor concentration, R_0, was held constant, and nonlinear least squares estimates were determined for the affinity of receptor for cofactor in the absence of ligand (K_d), the affinity of the ligand for receptor in the absence of cofactor (K_L), and the ratio of cofactor affinities in the absence and presence of ligand (α).

Transfections and Cell Culture/Plasmid Constructs. Expression plasmids for the VP16-human PPAR constructs were prepared by inserting amplified cDNAs encoding full-length PPARα, PPARγ2, and PPARδ fused to amino acids 410−490 of the VP16 viral activation domain into the expression vector pVP16 (Clonetech). GAL4DBD-CBP (1−115), GAL4DBD-NCoR (2012−2103), and GAL4DBD-NCoR (2239−2300) were generated by insertion of PCR amplified cDNAs encoding the indicated amino acids fused into a modified GAL4 DNA-binding domain (amino acids 1−147). The reporter plasmid was $(UAS)_5$-tk-SPAP (secreted placental alkaline phosphatase), and the internal control plasmid for all transfections was β-galactosidase expression vector (pCH110, Amersham).

Mammalian Two-Hybrid Assay. CV-1 cells were cultured in DME high glucose media supplemented with 10% FBS and 2 mM glutamine in a humidified incubator (5% CO_2 in air) at 37 °C. Three days prior to plating for transfection, cells were harvested with 0.25% trypsin/2 mM EDTA in phenol red-free Dulbecco's phosphate buffered saline (without calcium or magnesium) and collected in phenol red-free DMEM-F12/15 mM HEPES medium supplemented with 10% charcoal/dextran treated fetal bovine serum and 2 mM L-glutamine (experimental medium). Following 3 days in culture, cells were again harvested and suspended in experimental medium. The cells were seeded at 2.0×10^4 cells per well in a 96-well plate and returned to the incubator for 24 h. Cells were then transfected using Lipofectamine (Life Technologies, Inc.) according to the manufacturer's instructions. The total amount of DNA transfected into each well was 80 ng. Transfection mixtures contained 8 ng of VP16-PPAR plasmid, 8 ng of SPAP reporter, 25 ng of pCH110-β-gal control plasmid, 35 ng of pBluescript II KS+ (Clonetech), and 4 ng of either coactivator or corepressor plasmid. Transfection quantities for full-length PPAR and cofactor plasmids were optimized to generate a signal that was half of the total activation. These conditions would allow for dissociation or association to be experimentally determined for each ligand evaluated. Cells were transfected for 16 h, the medium was aspirated, and 100 μL of ligand was added. Appropriate ligand concentrations were prepared from DMSO stock solutions using phenol red-free DMEM/F-12 supplemented with 10% heat-inactivated, delipidated, charcoal-stripped FBS. The final concentration of DMSO was 0.1%. Cells were incubated for 24 h in the presence of drug, after which the media was sampled and assayed for alkaline phosphatase activity, and the cells were assayed for β-galactosidase activity to normalize for transfection efficiency. Plates were read on a Thermomax platereader (Molecular Devices) at 405 nM.

All determinations were performed at a minimum in triplicate, and the statistical significance of interaction in the presence of ligand with respect to vehicle was assessed with Dunnett's multiple comparisons test using Version 4.04 of JMP Statistical Discovery Software (SAS Institute, Cary, NC).

Structural Determination of PPARa/SMRT/GW7845 Structure. The crystallization conditions, data collection, structure determination, and refinement were as described previously (*32*). The structure was solved to a 3.2 Å resolution.

Molecular Modeling. X-ray structures of GW6471 and GW7845 bound to repressed conformations of PPARα and of GI262570, GW9544, and GW2433 bound to active conformations of PPARγ, PPARα, and PPARδ, respectively (*33*, *35*, *36*) were rotated to a common orientation with the MVP program (*43*). The GW7845 molecule from the PPARα X-ray structure was then docked into the active conformations of PPARγ, PPARα, and PPARδ by rigid superimposition onto corresponding atoms of the rotated GI262570, GW9544, and GI262570, respectively. The pocket depiction in Figure 8 was obtained by flooding the ligand binding pocket with closely spaced water-sized spheres using the MVP program and then generating a translucent Connolly surface to cover the spheres.

RESULTS

Measurement of TRβ LBD/Cofactor Peptide Interactions by Fluorescence Polarization. We have developed a fluorescence polarization assay to quantitatively measure the binding affinities of corepressor motifs for various nuclear receptor LBDs. This is done using fluorescently labeled corepressor peptides derived from the C-terminal nuclear receptor binding site(s) of NCoR and SMRT, which contain the LXXXIXXX(L/I) motif essential for nuclear receptor

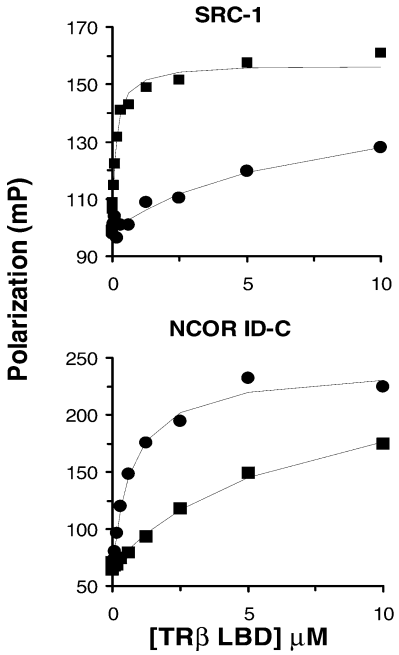

FIGURE 1: Fluorescence polarization assay for ligand modulation of TRβ LBD/cofactor peptide affinities. The effects of no compound (●) or 20 μM T3 (■) on the binding of the thyroid receptor-β LBD to a SRC-1 or NCoR peptide are shown. Complex formation was monitored by fluorescence polarization as described in the Materials and Methods. Each data point is the average of at least two independent experiments. Apparent affinities for the SRC-1 and NCoR peptides in the absence of ligand are 7.1 ± 4.0 and 0.72 ± 0.1 μM, respectively. In the presence of T3, the affinities are 0.13 ± 0.02 μM for SRC-1 and 6.2 ± 1.0 μM for NCoR.

binding. In addition, a linked equilibrium between nuclear receptor/cofactor interaction and the binding of ligand is well-established, such that the binding of ligand can alter the binding affinity for nuclear receptor/coregulator (*44*). Therefore, we also wanted to test whether the cofactor peptides could be used to replicate the ligand-induced effects observed for the nuclear receptor/coregulator interactions in cellular and in vitro assays. This is done by measuring the effect of ligand on the binding of the corepressor peptide. Corepressor binding is well-characterized in the literature for the thyroid receptor, in which the natural ligand causes displacement of the corepressor and recruitment of the coactivator. As seen in Figure 1, increasing concentrations of the TRβ LBD increase the polarization of the fluorescent LXXLL-containing peptides from the coactivator SRC-1 and corepressor NCoR, indicative of binding of the peptides to the receptor. In the absence of ligand, the TRβ LBD has a higher apparent affinity for the NCoR corepressor peptide (0.72 ± 0.08 μM) than with the SRC-1 coactivator peptide (7.1 ± 4.0 μM). Addition of the agonist ligand T3 increases the apparent affinity of the receptor SRC-1 interaction 50-fold to 130 nM but weakens the affinity of the receptor-NCoR ID-C interaction 9-fold to 6.2 μM. In the absence of ligand, the TRβ LBD had a 10-fold greater affinity for the corepressor peptide than coactivator peptide. Yet in the presence of the agonist ligand T3, this preference is reversed with the TRβ LBD having a 48-fold greater affinity for coactivator peptide than corepressor peptide. These results quantitatively demonstrate how ligand-induced changes in affinity for the coactivator and corepressor motifs can result in exchange of corepressors for coactivators as is seen in a biological context. Therefore, although other regions of nuclear receptor, cofactor, or other ancillary factors may be involved in their in vivo interaction, cofactor peptides can be used to quantitatively study the specific interaction between the corepressor motif and the coregulator binding surface of the nuclear receptor LBD.

Effect of Ligands on PPAR LBDs Binding to NCoR and SMRT Corepressor Peptides. We applied the fluorescence polarization assay described above to evaluate the effects of PPAR ligands on the binding of the three PPAR subtype LBDs to corepressor motifs from NCoR and SMRT. As seen in Figure 2, the highest affinity in the absence of ligand for the NCoR peptide is observed with the PPARγ LBD (1.7 μM), while both PPARα (5.0 μM) and PPARδ (6.0 μM) have somewhat weaker affinities. Little or no differences (within the error) are observed for the corresponding SMRT ID-C peptide.

We next examined the effects on corepressor peptide affinities of ligands (Figure 3), which selectively activate PPARγ in cell-based assays. The TZD rosiglitazone and L-tyrosine-based GW1929 and GW7845 have been considered PPARγ specific compounds since they have much weaker affinities for PPARα or PPARδ in cell-based functional assays (*1*). As is expected with classical agonists, all three of these ligands reduce the apparent affinity of PPARγ for both the NCoR and the SMRT corepressor peptides (Figure 2C,D).

With PPARα and PPARδ, the TZD rosiglitazone had little or no effect on the interactions with the corepressor peptides (Figure 2). Surprisingly, with PPARδ, the L-tyrosine compounds GW1929 and GW7845 increase the apparent affinity of PPARδ for the corepressor peptides (Figure 2E,F). With PPARα, only GW7845 appears to enhance the affinity for the corepressor peptides (Figure 2A,B). Therefore, we have identified ligands that weaken the affinity of corepressor peptides for PPARγ but have the opposite effect and enhance the affinity on PPARδ (GW7845 and GW1929) and in one case enhance the affinity of both PPARα and PPARδ (GW7845).

Effect of Compound Classes on Coregulator Peptide Affinity for PPAR Subtype LBDs. Differences in subtype compound affinities and different cofactor affinities complicate quantitative comparisons of the effect of ligands on PPAR subtypes. Therefore, we have developed a method of analysis that allows us to determine the quantitative effects of ligands on cofactor affinity regardless of the ligand and cofactor concentrations used in a particular experiment. The quantitative effects of compounds on coactivator/corepressor affinity were profiled via a fluorescence resonance energy transfer (FRET) assay. Biotinylated coactivator fragments derived from CBP (amino acids 57−454) and a corepressor peptide (NCoR ID-C) were labeled with europium-conjugated steptavidin. Biotinylated PPAR LBDs were labeled with allophycocyanin-conjugated steptavidin. The effect of compounds on the binding of each PPAR subtype LBD to a fragment of CBP or the NCoR ID-C peptide were determined by varying the ligand concentration in the presence of 10 nM PPAR LBD and four different concentrations of CBP and NCoR. The data for the effect of the tyrosine-based ligand GW1929 on PPARγ binding to the CBP and the NCoR peptide are shown in Figure 4. The data were simultaneously fit to an interaction model described in the Materials and Methods and the Supporting Information. The

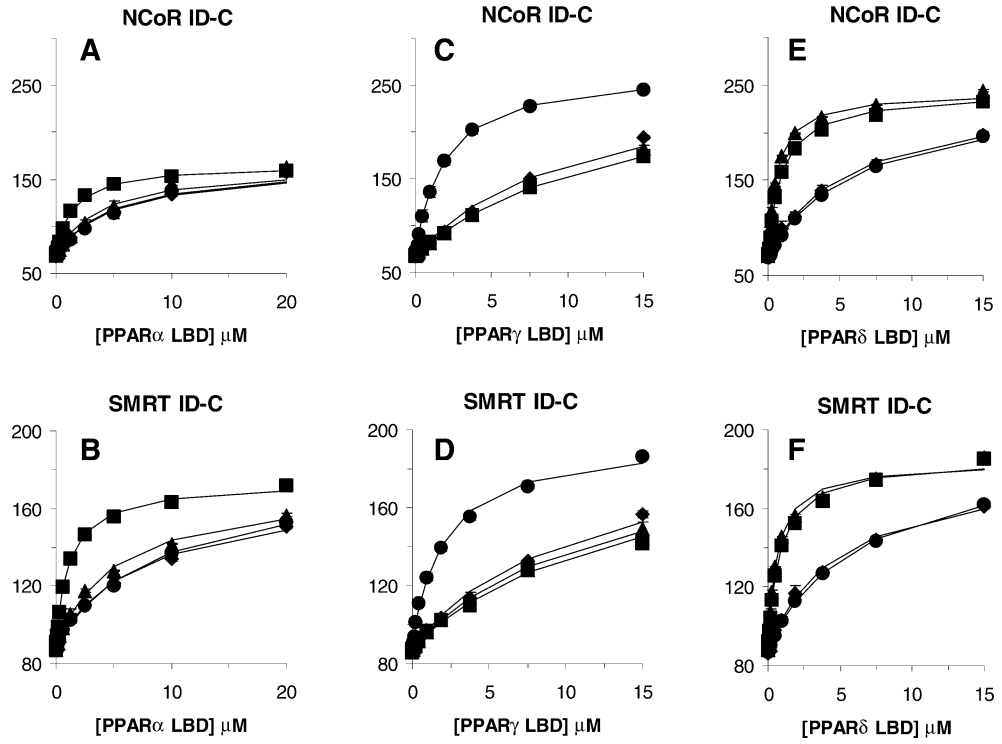

FIGURE 2: Fluorescence polarization assay for ligand modulation of PPAR/corepressor peptide binding. The effects of no compound (●), 40 μM GW1929 (▲), 40 μM GW7845 (■), or 40 μM rosiglitazone (◆) on the binding of the three PPAR subtype LBDs to 10 nM fluorescein-NCoR ID-C peptide or 10 nM fluorescein-SMRT ID-C peptide are shown. Complex formation was monitored by fluorescence polarization as described in the Materials and Methods. Each data point is the average of at least two independent determinations with error bars corresponding to the standard deviation. Apparent K_D values (± standard deviation) of PPARα for fluorescein-NCoR ID-C peptide are 4.9 ± 0.8 μM (no ligand), 3.8 ± 0.9 μM (GW1929), 1.4 ± 0.4 μM (GW7845), and 4.8 ± 0.6 μM (rosiglitazone). Apparent K_D values (± standard deviation) of PPARγ for fluorescein-NCoR ID-C peptide are 1.7 ± 0.3 μM (no ligand), 12 ± 1.1 μM (GW1929), 13 ± 1.5 μM (GW7845), and 10.3 ± 0.5 μM (rosiglitazone). Apparent K_D values (± standard deviation) of PPARδ for fluorescein-NCoR ID-C peptide are 6.0 ± 0.9 μM (no ligand), 0.62 ± 0.06 μM (GW1929), 0.8 ± 0.06 μM (GW7845), and 5.5 ± 1.9 μM (rosiglitazone). Apparent K_D values (± standard deviation) of PPARα for fluorescein-SMRT ID-C peptide are 7.0 ± 2.1 μM (no ligand), 5.1 ± 0.1 μM (GW1929), 1.1 ± 0.05 μM (GW7845), and 6.9 ± 1.4 μM (rosiglitazone). Apparent K_D values of PPARγ for fluorescein-SMRT ID-C peptide are 2.1 ± 0.3 μM (no ligand), 12 ± 0.6 μM (GW1929), 9.5 ± 3.4 μM (GW7845), and 12 ± 2 μM (rosiglitazone). Apparent K_D values (± standard deviation) of PPARδ for fluorescein-SMRT ID-C peptide are 5.2 ± 0.4 μM (no ligand), 0.69 ± 0.03 μM (GW1929), 0.85 ± 0.1 μM (GW7845), and 4.8 ± 0.5 μM (rosiglitazone).

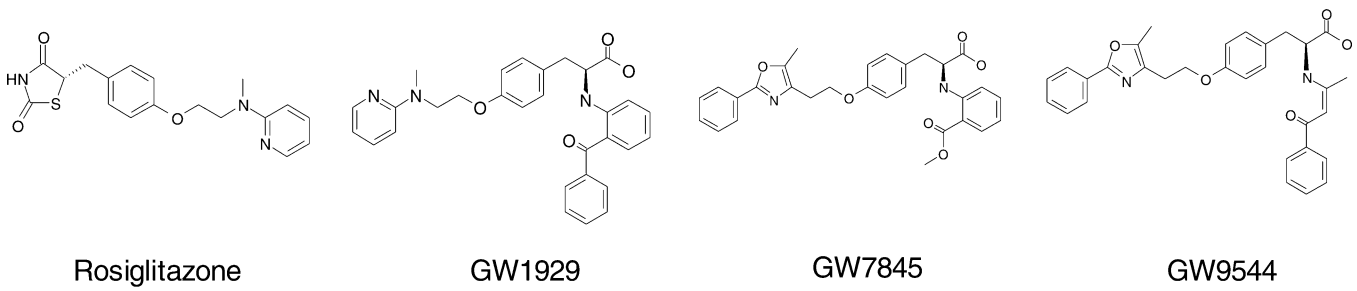

FIGURE 3: Structures of PPAR compounds.

experimentally determined α value is the ratio of cofactor affinities in the absence and presence of a saturating concentration of ligand. This analysis permits a direct comparison of the effects of compounds, independent of cofactor concentration and differences in coregulator affinity for the individual receptors. Fitted parameters for PPARγ/CBP/GW1929 interaction were calculated to be 7.9 nM for the affinity of the ligand in the absence of cofactor (K_L) and an α value of 23, indicating that the apparent affinity of GW1929 for PPARγ in the presence of saturating CBP (K_L/α) would be 0.34 nM. For the PPARγ/NCoR/GW1929 complex, the α value is calculated to be 0.05, yielding a value for the apparent affinity of GW1929 for PPARγ in the presence of saturating NCoR to be 158 nM. Therefore, GW1929 behaves as a classical agonist with PPARγ by enhancing the affinity for a coactivator and reducing the affinity for corepressor.

A diverse set of PPAR ligands was analyzed as above using the FRET assay, and the α values for each compound on each receptor subtype were determined. The α values are plotted in Figure 5 as log(α) such that a ligand that increases the affinity for cofactor is greater than zero, and a decrease in affinity is less than zero, which facilitates the comparison of the ligand responses. As seen in Figure 5, the TZDs (rosiglitazone and pioglitazone) as well as tyrosine-based PPARγ activators (GW1929 and GW7845) and the PPARδ ligand (GW1516) (*8*) increase the apparent affinity of all three PPAR subtypes for the coactivator fragment from CBP.

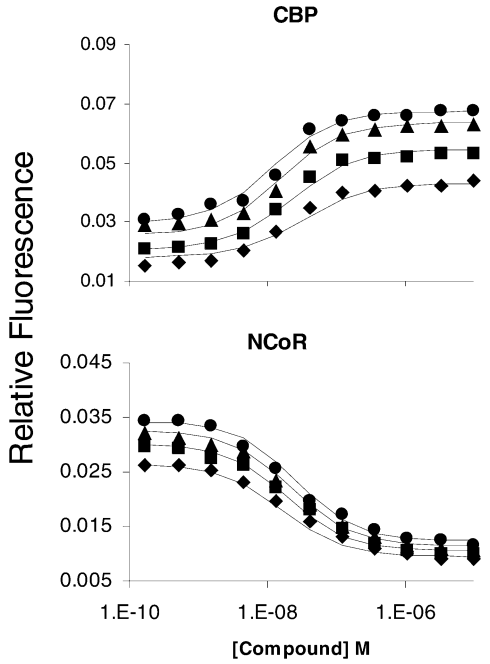

FIGURE 4: GW1929 modulation of PPARγ cofactor complexes. The effect of GW1929 on 10 nM PPARγ LBD binding to CBP (57−454) or NCoR ID-C peptide was determined by time-resolved fluorimetry as described in the Materials and Methods. The relative fluorescence is the ratio of the fluorescence intensity at 665 and 610 nm. Concentrations of CBP were 25 nM (◆), 50 nM (■), 100 nM (▲), and 150 nM (●). Concentrations of NCoR ID-C are 100 nM (◆), 150 nM (■), 200 nM (▲), and 250 nM (●).

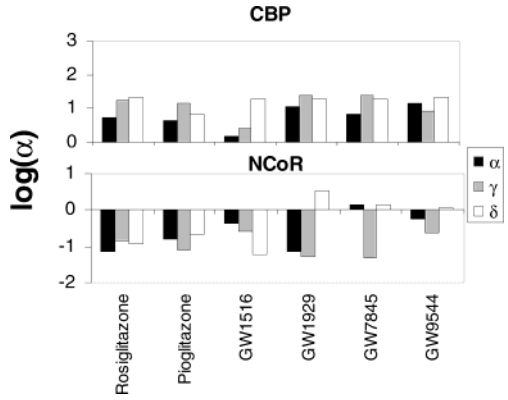

FIGURE 5: Effect of ligands on coactivator and corepressor binding to PPAR subtypes determined by FRET. The fold increases in affinity (α) of various ligands on PPAR subtype binding to a fragment of CBP (57−454) or the NCoR ID-C peptide were determined by fluorescence energy transfer (FRET) as described in the Materials and Methods.

Although quantitative differences in the enhancement of binding are observed, particularly for the PPARδ compound GW1516, the diverse PPAR agonists each appear to exert increases in affinity for the coactivator regardless of receptor subtype. In contrast, the ligands exert varied PPAR subtype-dependent effects on the affinities for the corepressor peptide. For example, TZD compounds and the PPARδ ligand, GW1516, decrease the affinity of all three subtypes for the corepressor peptide as expected of classical agonists. In contrast, the tyrosine-based ligands decrease the affinity for PPARγ for the corepressor peptide but have little effect, or modestly enhance the affinity of PPARδ for the corepressor peptide. GW1929 shows the greatest enhancement of corepressor binding to PPARδ. For PPARα, only GW7845 shows

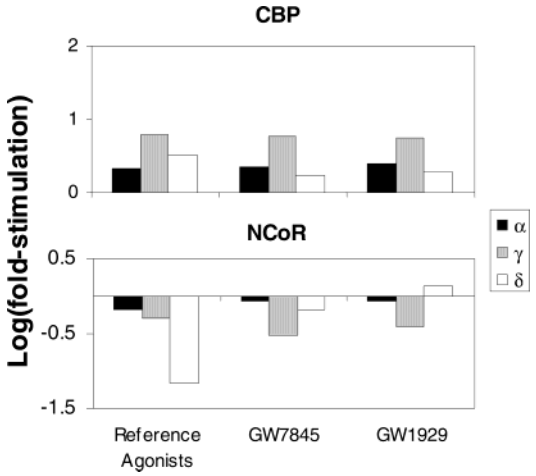

FIGURE 6: Characterization of ligand effects on PPAR/cofactor interactions in a cell-based assay. Complex formation was evaluated using a mammalian two-hybrid interaction assay with full-length PPAR receptors and cofactor fragments as described in the Materials and Methods. The effect of 10 μM of the indicated compound on VP16 full-length PPARα, PPARγ, or PPARδ binding to GAL4DBD-CBP or GAL4DBD-NCoR 2239−2300 is shown. Reference agonists were GW9820x for PPARα, pioglitazone for PPARγ, and GW1514 for PPARδ. Values determined for each ligand were significantly different from vehicle as determined by with Dunnett's multiple comparisons test at $p < 0.01$.

a modest but detectable enhancement in binding of the corepressor peptide. Taken together, these experiments demonstrate overall profiles where different compounds have varied effects on both the direction and the magnitude of corepressor binding among the three PPAR subtypes.

Effect of Tyrosine Class of PPAR Ligands on Coactivator and Corepressor Binding to Full-Length Receptor in a Mammalian Two-Hybrid Assay. A mammalian two-hybrid assay was used to examine the ability of the tyrosine-based class of PPAR ligands to promote association or dissociation of the coactivator CBP and the corepressor NCoR in the context of a cellular environment. The assay uses full-length human PPARα, PPARγ2, and PPARδ fused to the activation domain of VP16 and previously identified interaction domains of CBP and NCoR fused to the DNA binding domain of GAL4. This assay was optimized with the intent to demonstrate ligand-dependent association or dissociation to full-length PPARs by coregulators. Thus, the total fold activation was not as high as described in other assays. Using full-length PPAR subtypes, three reference agonists (GW9820, pioglitazone, and GW1514 for PPARα, PPARγ, and PPARδ, respectively) exhibited a classical agonist profile in which they promote the association of a fragment of CBP (Figure 6) and reduce the association with corepressor interaction domain (2239−2300) containing NCoR ID-C (Figure 6). None of the PPAR subtypes interacted with a NCoR fragment (2012−2103) that contained NCoR ID-N (data not shown). The tyrosine-based ligand, GW1929, reduces association of NCoR with PPARγ and enhances its association with PPARδ while having little or no effect on PPARα. These results are consistent with the FRET assays (Figure 5). The ligand GW7845 inhibited binding of NCoR to PPARγ but appears to modestly reduce binding of NCoR to PPARα and PPARδ, unlike the cell-free assays where modest increases in NCoR binding are observed (Figure 5). Nevertheless, we observe similar qualitative effects of ligands

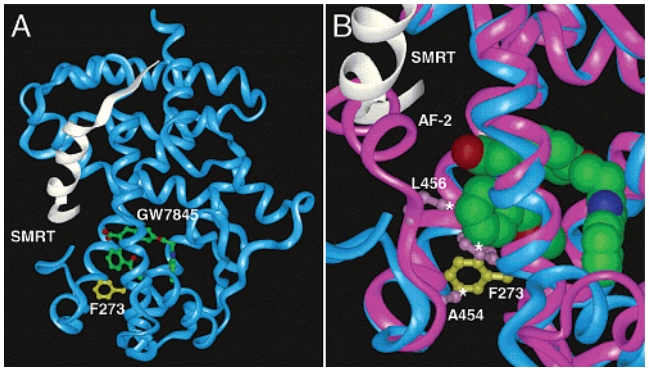

FIGURE 7: X-ray crystal structure of PPARα LBD/GW7845/SMRT peptide complex. (A) An overview of the PPARα/SMRT/GW7845 complex. The PPARα LBD and SMRT peptide are epicted as blue and white worms, respectively, while GW7845 and key protein residues are shown in a ball-and-stick representation. (B) Superposition of the GW7845-bound PPARα/SMRT structure (blue and white worms) onto the previously described GW9544-PPARα/SRC-1 complex (magenta worm) (*32*). Key side chains in the GW7845 and GW9544 structures are shown in yellow and pink, respectively. The benzene ring of GW7845 would bump against L456 and F273, pushing the latter side chain against A454, as denoted by white stars, if the protein retained the fully active conformation of the GW9544 structure.

on corepressor binding to those observed in the more quantitative cell-free assays such that the peptides derived from defined coactivator and corepressor interaction domains are tools that can be used to model ligand-dependent coregulator modulation of PPAR interaction in a cellular context.

Structural Basis of GW7845 and GW1929 Effects on Corepressor Affinity with PPARα and PPARδ. A potential explanation for the subtype-dependent effects of the tyrosine-based ligands on PPAR/corepresor affinity is revealed by the crystal structure of the PPARα/GW7845/SMRT complex (Figure 7A). This structure was solved by molecular replacement using the PPARα/GW6471/SMRT structure as a model (*36*). It is remarkably similar to the previously described PPARα/corepressor structure, with the corepressor peptide forming a three-turn α-helix that fits into the same groove as the coactivator motif, thereby preventing the carboxy-terminal activation helix (AF2) from adopting its active conformation.

Figure 7B depicts the active PPARα/SRC-1/GW9544 structure (*36*) overlaid onto the repressed PPARα/SMRT/GW7845 structure. This overlay shows that the acidic headgroup of GW7845 is oriented toward the active position of the AF2 helix, as occurs with GW9544, where it could make the hydrogen bonding interaction with Tyr464 that normally stabilizes the AF2 helix, thereby promoting coactivator binding. However, the overlay also shows that if PPARα adopted the active conformation of the GW9544 complex, then the bulky benzene group of GW7845 would bump Leu456 and Phe273, pushing the latter residue against Ala454. As is observed in Figure 7B, these steric clashes appear to shift the AF2 linker into conformations that disturb the active position of the AF2 helix and therefore enhance corepressor binding. However, there is no steric clash with the AF2 helix itself, and the linker is free to assume other conformations that could place the AF2 helix in the active position in the presence of coactivator. Thus, GW7845 makes interactions with PPARα that promote binding of coactivator

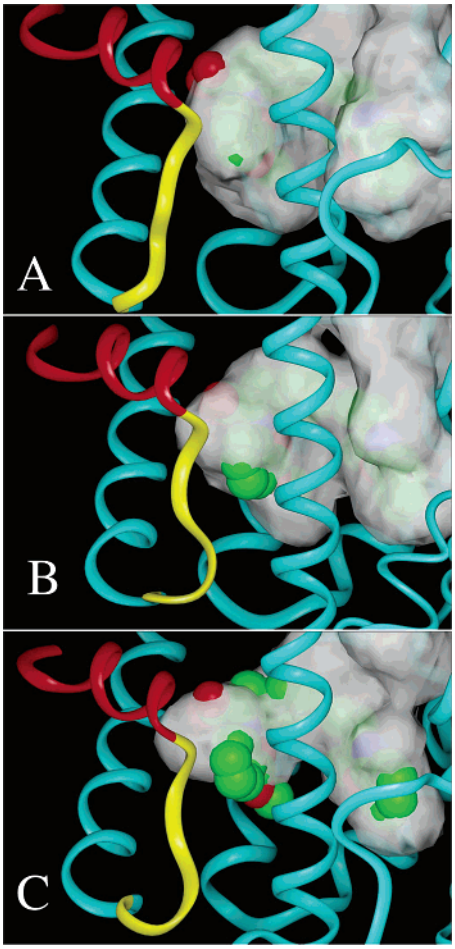

FIGURE 8: Models of GW7845 bound to each of the three PPAR subtypes in their active conformations. The ligand GW7845 was modeled into X-ray structures for the active conformations of (A) PPARγ, (B) PPARα, and (C) PPARδ. In each case, the ligand is shown in a space-filling representation, with atoms colored green, blue, and red for carbon, nitrogen, and oxygen, respectively. The protein is depicted in a worm representation, colored red for the AF2 helix, yellow for the AF2 linker, and cyan elsewhere. The solvent-accessible ligand binding pocket is represented by a translucent white surface.

as well as corepressor. By contrast, the conventional antagonist GW6471 clashes directly with the AF2 helix, thereby preventing coactivator binding and promoting corepressor binding (*36*).

The PPARα/SMRT/GW7845 structure suggests that the subtype-dependent effects of ligands on coactivator and corepressor affinity can be rationalized in terms of the differential ligand fit into the ligand binding pockets of the three PPAR subtypes. The GW7845 methyl ester group necessarily fits into the benzophenone pocket formed by helices 3, 6, and 10 and the AF2 linker (*33*). The benzophenone pocket is largest and widest in PPARγ, somewhat smaller in PPARα, and substantially smaller in PPARδ (*36*). As discussed previously (*36*), PPARγ can easily accommodate the bulk of a benzophenone group or the similar benzene methyl ester, whereas PPARα cannot. Other compounds with narrower substituents at this position, such as GW9544 (Figure 3), can bind with high affinity to both PPARγ and PPARα (*36*). Figure 8A depicts the situation for PPARγ, showing that the GW7845 ligand is easily accommodated within the white surface representing the volume available to ligand in PPARγ. In contrast, the

benzene methyl ester group of GW7845 protrudes through the PPARα benzophenone pocket (Figure 8B), consistent with the structural results in Figure 7. The benzophenone pocket is further narrowed in PPAR*δ*, partly because of substitution of Met355 in PPARα with an isoleucine. Therefore, GW7845 protrudes even more dramatically through the PPAR*δ* benzophenone pocket surface, as is observed in Figure 8C. Consistent with the smaller pocket shape of PPAR*δ*, GW1929, GW7845, and even the narrower ligand GW9544 appear to enhance binding of corepressor to PPAR*δ* (Figures 2 and 5). Interestingly, GW1929 does not appear to enhance corepressor affinity on PPARα (Figures 2 and 5), even though it has a bulky benzophenone group at the N-substituent position similar to the benzene methyl ester in GW7845 (Figure 3). This may be due to the shorter amino-pyridine tail in GW1929, which leaves room for the PPARα protein to better accommodate the extra bulk of the benzophenone group without destabilizing the AF2 helix. These observations suggest that for PPARα and PPAR*δ* to accommodate the large substituents of some of the tyrosine-based ligands, rearrangements of the ligand binding pocket are required that result in altered presentations of the overlapping coactivator/corepressor binding surface.

DISCUSSION

Current models of nuclear receptor mediated gene activation suggest that ligands can activate a nuclear receptor by promoting the dissociation of a corepressor complex and enhancing the formation of a coactivator complex. The structural basis for this is revealed by numerous coactivator structures (for review, see ref *45* and the recently solved PPARα/antagonist/corepressor structure (*32*)). These studies indicate that for PPARs, the position of the AF2 helix is the primary determinant of whether a nuclear receptor is in the active or inactive conformation. Ligands that stabilize the AF2 helix in an active conformation enhance the affinity for LXXLL-containing coactivator sequences, thereby leading to receptor activation. Since the active position of the AF2 helix and the extended helix of the corepressor motif overlap, their binding is mutually exclusive such that ligands that stabilize the AF2 helix in the active position would be expected to reduce the affinity for corepressor. Conversely, ligands that favor the AF2 helix in a position other than the active conformation may enhance the affinity for corepressor motifs and reduce the affinity for coactivator motifs, thereby diminishing the basal activity of the receptor. This analysis indicates that ligands could be identified that redistribute the equilibrium of the AF2 helix among multiple conformations, therefore altering the affinities and preferences for coregulators over a wide range and resulting in differential receptor activation or repression. This concept is supported by recent work that identified specific phage peptides that only recognize ER in the presence of specific ligands (*46*). These phage peptides are likely detecting ligand-induced changes in receptor conformation that could potentially be recognized by different coregulator proteins. These observations suggest that novel ligands can be identified that stabilize a continuum of conformational states in nuclear receptors resulting in varied degrees of receptor activation or repression.

To identify and characterize ligands with diverse effects on receptor conformation, we have developed biophysical techniques that measure the effects of ligands on the affinities of coactivator and corepressor peptides to PPAR subtypes. These techniques allow us to specifically and quantitatively assess the effect of a ligand on the coregulator binding surface of the LBD of the receptor in the absence of other endogenous receptors or cofactors that can complicate the interpretation of many cellular assays. We have applied these techniques to a panel of diverse PPAR ligands and find that the PPAR*γ*-directed thiazolidinediones (rosiglitazone and pioglitazone) and tyrosine-based ligands (GW1929 and GW7845) enhance the affinity for coactivators and decrease the affinity for corepressor on PPAR*γ*. This is the expected profile of a classical agonist. We previously described a PPARα ligand that enhanced corepressor binding and diminished coactivator binding that is the profile expected of a classical antagonist. (*32*) In contrast, we identified a novel ligand profile in which the tyrosine ligand (GW1929) promotes the binding of coactivator, but unlike a classical agonist has little effect or modestly enhances the affinity of corepressor peptides for PPAR*δ*. In addition, another tyrosine-based ligand GW7845 promotes the binding of coactivator and corepressor peptides to both PPARα and PPAR*δ*. These two tyrosine-based ligands exert unusual PPAR-subtype dependent, mixed agonist/antagonist properties in which they inhibit the binding of corepressor to one subtype but enhance the affinity for another. In addition, these ligands have the ability to enhance the binding of both coactivator or corepressor, such that these ligands would be expected to activate PPAR*δ* when the coactivator/corepressor ratio is high and repress the receptor when the ratio is low. Therefore, we have identified ligands that exert a range of effects on corepressor binding that could lead to a variety of biological activities.

The two tyrosine-based PPAR ligands that exhibited subtype-dependent effects on corepressor affinity are closely related structurally and both contain a bulky group at the N-substituent position not found in the TZDs (Figure 3). The structural studies presented here suggest that the PPAR subtype differences in the size of the benzophenone pocket formed by helices 3, 7, and 10 and the AF2 loop (*33*, *36*) are the molecular basis for the differential effects of these ligands on the binding of corepressors. This pocket in PPARα is somewhat smaller than in PPAR*γ* and significantly smaller in PPAR*δ*. We find that GW7845 and GW1929, which have a bulky group on the tyrosine nitrogen, can occupy the ligand pocket of PPARα and PPAR*δ* but only with significant alteration of the pocket. These ligands push against the side chains of the helix AF2 linker region that in turn promote the displacement of the AF2 helix from its active position. This mechanism of enhanced corepressor binding is different from previously described receptor antagonists in which a bulky ligand substituent protrudes out of the binding pocket and sterically prevents the AF2 helix from attaining its active conformation (*45*). We recently described the cocrystal structure of PPARα with an antagonist, GW6471, which contains a bulky headgroup that prevents the ligand from forming an activating hydrogen bond with the AF2 helix, resulting in reduced affinity for coactivator and enhanced affinity for corepressors (*32*). The structure of PPARα complexed with GW7845 shows that the ligand would not sterically prevent the AF2 helix from orienting in its active conformation, such that GW7845 could also enhance the binding of coactivators as was observed in

the peptide binding assays.

These studies demonstrate the dynamic nature of the ligand binding pockets of the PPARs, which allow them to accommodate a number of ligands. The binding of these ligands and the resulting modulation of receptor conformation can have differential effects on the coactivator/corepressor binding surface and therefore can influence the biological activity of these ligands. The biological effects of a ligand on a specific nuclear receptor depend not only on the intrinsic affinity of the ligand for the receptor but also on the coregulator context of the target cell. This coregulator context involves both the types of coactivators and corepressors as well as the relative levels/concentrations of these coregulators, which likely varies significantly among cell and tissue types. Therefore, ligands with differential effects on corepressor binding could have tissue-dependent effects depending on the coregulator environment of the host cell. One example of this is the search for selective estrogen receptor modulators (SERMs) that have the desired positive bone/cardiovascular effects, without the unwanted proliferative effects in breast and uterine tissues (*47*). It has recently been suggested that tissue differences in the levels of coregulators are responsible for the tissue selectivity of SERMs such as tamoxifen (*48*) and partial agonist activity of RU486 with the progesterone receptor (*49*). Therefore, ligand profiling with both coactivator and corepressor that we have described is an important step in identifying and characterizing novel ligands with desired biological activities. We believe the challenge now is to design ligands with multiple profiles and identify which ligand profiles correlate with the desired physiological/biological outcome.

In summary, we have developed biophysical techniques to characterize the interaction of both coactivators and corepressors with nuclear receptors that allows us to quantitatively profile the effects of ligands on this interaction. We have used these assays to identify ligands that have an unexpected and previously unseen profile in which a ligand can promote the binding of both coactivator and corepressor proteins. In addition, we have identified structural differences in the ligand binding pockets of the three PPAR subtypes that appear to be responsible for this novel coactivator/corepressor profile. These observations provide new insight into the mechanism of corepressor binding, differential effects on coregulator binding by various ligands, and structural variations that can lead to altered presentation of the coregulator binding surface.

ACKNOWLEDGMENT

The authors thank Thomas G. Consler and G. Bruce Wisley for initial preparation of PPAR constructs, Randy K. Bledsoe for preparation of the CBP construct, William Burkhardt and Mary Moyer for protein sequencing and amino acid analysis, and Timothy Willson for critical review of the manuscript.

SUPPORTING INFORMATION AVAILABLE

FRET data analysis. This material is available free of charge via the Internet at http://pubs.acs.org.

REFERENCES

1. Willson, T. M., Brown, P. J., Sternbach, D. D., and Henke, B. R. (2000) *J. Med. Chem. 43*, 527−550.
2. Issemann, I., and Green, S. (1990) *Nature 347*, 645−650.
3. Lehmann, J. M., Moore, L. B., Smith-Oliver, T. A., Wilkison, W. O., Willson, T. M., and Kliewer, S. A. (1995) *J. Biol. Chem. 270*, 12953−12956.
4. Henke, B. R., Blanchard, S. G., Brackeen, M. F., Brown, K. K., Cobb, J. E., Collins, J. L., Harrington, W. W., Jr., Hashim, M. A., Hull-Ryde, E. A., Kaldor, I., Kliewer, S. A., Lake, D. H., Leesnitzer, L. M., Lehmann, J. M., Lenhard, J. M., Orband-Miller, L. A., Miller, J. F., Mook, R. A., Jr., Noble, S. A., Oliver, W., Jr., Parks, D. J., Plunket, K. D., Szewczyk, J. R., and Willson, T. M. (1998) *J. Med. Chem. 41*, 5020−5036.
5. Collins, J. L., Blanchard, S. G., Boswell, G. E., Charifson, P. S., Cobb, J. E., Henke, B. R., Hull-Ryde, E. A., Kazmierski, W. M., Lake, D. H., Leesnitzer, L. M., Lehmann, J., Lenhard, J. M., Orband-Miller, L. A., Gray-Nunez, Y., Parks, D. J., Plunkett, K. D., and Tong, W. Q. (1998) *J. Med. Chem. 41*, 5037−5054.
6. Cobb, J. E., Blanchard, S. G., Boswell, E. G., Brown, K. K., Charifson, P. S., Cooper, J. P., Collins, J. L., Dezube, M., Henke, B. R., Hull-Ryde, E. A., Lake, D. H., Lenhard, J. M., Oliver, W., Jr., Oplinger, J., Pentti, M., Parks, D. J., Plunket, K. D., and Tong, W. Q. (1998) *J. Med. Chem. 41*, 5055−5069.
7. Brown, K. K., Henke, B. R., Blanchard, S. G., Cobb, J. E., Mook, R., Kaldor, I., Kliewer, S. A., Lehmann, J. M., Lenhard, J. M., Harrington, W. W., Novak, P. J., Faison, W., Binz, J. G., Hashim, M. A., Oliver, W. O., Brown, H. R., Parks, D. J., Plunket, K. D., Tong, W. Q., Menius, J. A., Adkison, K., Noble, S. A., and Willson, T. M. (1999) *Diabetes 48*, 1415−1424.
8. Oliver, W. R., Jr., Shenk, J. L., Snaith, M. R., Russell, C. S., Plunket, K. D., Bodkin, N. L., Lewis, M. C., Winegar, D. A., Sznaidman, M. L., Lambert, M. H., Xu, H. E., Sternbach, D. D., Kliewer, S. A., Hansen, B. C., and Willson, T. M. (2001) *Proc. Natl. Acad. Sci. U.S.A. 98*, 5306−5311.
9. Zhu, Y., Qi, C., Calandra, C., Rao, M. S., and Reddy, J. K. (1996) *Gene Expression 6*, 185−195.
10. DiRenzo, J., Soderstrom, M., Kurokawa, R., Ogliastro, M. H., Ricote, M., Ingrey, S., Horlein, A., Rosenfeld, M. G., and Glass, C. K. (1997) *Mol. Cell. Biol. 17*, 2166−2176.
11. Dowell, P., Ishmael, J. E., Avram, D., Peterson, V. J., Nevrivy, D. J., and Leid, M. (1997) *J. Biol. Chem. 272*, 33435−33443.
12. Zhu, Y., Qi, C., Jain, S., Rao, M. S., and Reddy, J. K. (1997) *J. Biol. Chem. 272*, 25500−25506.
13. Yuan, C. X., Ito, M., Fondell, J. D., Fu, Z. Y., and Roeder, R. G. (1998) *Proc. Natl. Acad. Sci. U.S.A. 95*, 7939−7944.
14. Darimont, B. D., Wagner, R. L., Apriletti, J. W., Stallcup, M. R., Kushner, P. J., Baxter, J. D., Fletterick, R. J., and Yamamoto, K. R. (1998) *Genes Dev. 12*, 3343−3356.
15. Nolte, R. T., Wisely, G. B., Westin, S., Cobb, J. E., Lambert, M. H., Kurokawa, R., Rosenfeld, M. G., Willson, T. M., Glass, C. K., and Milburn, M. V. (1998) *Nature 395*, 137−143.
16. Alland, L., Muhle, R., Hou, H., Jr., Potes, J., Chin, L., Schreiber-Agus, N., and DePinho, R. A. (1997) *Nature 387*, 49−55.
17. Heinzel, T., Lavinsky, R. M., Mullen, T. M., Soderstrom, M., Laherty, C. D., Torchia, J., Yang, W. M., Brard, G., Ngo, S. D., Davie, J. R., Seto, E., Eisenman, R. N., Rose, D. W., Glass, C. K., and Rosenfeld, M. G. (1997) *Nature 387*, 43−48.
18. Nagy, L., Kao, H. Y., Chakravarti, D., Lin, R. J., Hassig, C. A., Ayer, D. E., Schreiber, S. L., and Evans, R. M. (1997) *Cell 89*, 373−380.
19. Glass, C. K., Rose, D. W., and Rosenfeld, M. G. (1997) *Curr. Opin. Cell Biol. 9*, 222−232.
20. Xu, L., Glass, C. K., and Rosenfeld, M. G. (1999) *Curr. Opin. Gen. Dev. 9*, 140−147.
21. Robyr, D., Wolffe, A. P., and Wahli, W. (2000) *Mol. Endocrinol. 14*, 329−347.
22. Chen, J. D., and Evans, R. M. (1995) *Nature 377*, 454−457.
23. Lavinsky, R. M., Jepsen, K., Heinzel, T., Torchia, J., Mullen, T. M., Schiff, R., Del-Rio, A. L., Ricote, M., Ngo, S., Gemsch, J., Hilsenbeck, S. G., Osborne, C. K., Glass, C. K., Rosenfeld, M. G., and Rose, D. W. (1998) *Proc. Natl. Acad. Sci. U.S.A. 95*, 2920−2925.
24. Hong, S.-H., David, G., Wong, C.-W., Dejean, A., and Privalsky, M. L. (1997) *PNAS 94*, 9028−9033.
25. Grignani, F., De Matteis, S., Nervi, C., Tomassoni, L., Gelmetti, V., Cioce, M., Fanelli, M., Ruthardt, M., Ferrara, F. F., Zamir, I., Seiser, C., Lazar, M. A., Minucci, S., and Pelicci, P. G. (1998) *Nature 391*, 815−818.
26. Yamamoto, Y., Wada, O., Suzawa, M., Yogiashi, Y., Yano, T., Kato, S., and Yanagisawa, J. (2001) *J. Biol. Chem. 276*, 42684−42691.

27. Hu, X., and Lazar, M. A. (1999) *Nature 402*, 93−96.
28. Perissi, V., Staszewski, L. M., McInerney, E. M., Kurokawa, R., Krones, A., Rose, D. W., Lambert, M. H., Milburn, M. V., Glass, C. K., and Rosenfeld, M. G. (1999) *Genes Dev. 13*, 3198−3208.
29. Nagy, L., Kao, H. Y., Love, J. D., Li, C., Banayo, E., Gooch, J. T., Krishna, V., Chatterjee, K., Evans, R. M., and Schwabe, J. W. (1999) *Genes Dev. 13*, 3209−3216.
30. Webb, P., Anderson, C. M., Valentine, C., Nguyen, P., Marimuthu, A., West, B. L., Baxter, J. D., and Kushner, P. J. (2000) *Mol. Endocrinol. 14*, 1976−1985.
31. Cohen, R. N., Putney, A., Wondisford, F. E., and Hollenberg, A. N. (2000) *Mol. Endocrinol. 14*, 900−914.
32. Xu, H. E., Stanley, T. B., Montana, V. G., Lambert, M. H., Shearer, B. G., Cobb, J. E., McKee, D. D., Galardi, C. M., Plunket, K. D., Nolte, R. T., Moore, J. T., Kliewer, S. A., Stimmel, J. B., and Willson, T. M. (2002) *Nature 415*, 813−817.
33. Gampe, R. T., Jr., Montana, V. G., Lambert, M. H., Miller, A. B., Bledsoe, R. K., Milburn, M. V., Kliewer, S. A., Willson, T. M., and Xu, H. E. (2000) *Mol. Cell 5*, 545−555.
34. Uppenberg, J., Svensson, C., Jaki, M., Bertilsson, G., Jendeberg, L., and Berkenstam, A. (1998) *J. Biol. Chem. 273*, 31108−31112.
35. Xu, H. E., Lambert, M. H., Montana, V. G., Parks, D. J., Blanchard, S. G., Brown, P. J., Sternbach, D. D., Lehmann, J. M., Wisely, G. B., Willson, T. M., Kliewer, S. A., and Milburn, M. V. (1999) *Mol. Cell 3*, 397−403.
36. Xu, H. E., Lambert, M. H., Montana, V. G., Plunket, K. D., Moore, L. B., Collins, J. L., Oplinger, J., Kliewer, S. A., Gampe, R. T., McKee, D. D., Moore, J. T., and Willson, T. M. (2001) *PNAS 98*, 13919−13924.
37. Kliewer, S., Forman, B., Blumberg, B., Ong, E., Borgmeyer, U., Mangelsdorf, D., Umesono, K., and Evans, R. (1994) *PNAS 91*, 7355−7359.
38. Bramlett, K. S., Wu, Y., and Burris, T. P. (2001) *Mol. Endocrinol. 15*, 909−922.
39. Wong, C. W., Komm, B., and Cheskis, B. J. (2001) *Biochemistry 40*, 6756−6765.
40. Warnmark, A., Almlof, T., Leers, J., Gustafsson, J.-A., and Treuter, E. (2001) *J. Biol. Chem. 276*, 23397−23404.
41. Leesnitzer, L. M., Parks, D. J., Bledsoe, R. K., Cobb, J. E., Collins, J. L., Consler, T. G., Davis, R. G., Hull-Ryde, E. A., Lenhard, J. M., Patel, L., Plunket, K. D., Shenk, J. L., Stimmel, J. B., Therapontos, C., Willson, T. M., and Blanchard, S. G. (2002) *Biochemistry 41*, 6640−6650
42. Cohen, S. A., and Michaud, D. P. (1993) *Anal. Biochem. 211*, 279.
43. Lambert, M. H. (1997) Docking Conformationally Flexible Molecules Into Protein Binding Sites in *Practical Application of Computer-Aided Drug Design*, Marcel Dekker, New York.
44. Gee, A. C., Carlson, K. E., Martini, P. G. V., Katzenellenbogen, B. S., and Katzenellenbogen, J. A. (1999) *Mol. Endocrinol 13*, 1912−1923.
45. Bourguet, W., Germain, P., and Gronemeyer, H. (2000) *Trends Pharmacol. Sci. 21*, 381−388.
46. Paige, L. A., Christensen, D. J., Gron, H., Norris, J. D., Gottlin, E. B., Padilla, K. M., Chang, C. Y., Ballas, L. M., Hamilton, P. T., McDonnell, D. P., and Fowlkes, D. M. (1999) *Proc. Natl. Acad. Sci. U.S.A. 96*, 3999−4004.
47. Grese, T. A., and Dodge, J. A. (1998) *Curr. Pharm. Des. 4*, 71−92.
48. Shang, Y., and Brown, M. (2002) *Science 295*, 2465−2468.
49. Liu, Z., Auboeuf, D., Wong, J., Chen, J. D., Tsai, S. Y., Tsai, M.-J., and O'Malley, B. W. (2002) *PNAS 99*, 7940−7944.

BI034472C